Acetylene cyclotrimerization by early second-row transition metals in the gas phase. A theoretical study

ARTICLE *in* INORGANIC CHEMISTRY · JANUARY 2005

Impact Factor: 4.76

5 AUTHORS, INCLUDING:

Ivan Rivalta

Yale University

57 PUBLICATIONS **595** CITATIONS

SEE PROFILE

Nino Russo

Università della Calabria

511 PUBLICATIONS **7,939** CITATIONS

SEE PROFILE

Emilia Sicilia

Università della Calabria

151 PUBLICATIONS **1,943** CITATIONS

SEE PROFILE

Inorg. Chem. **2005**, *44*, 9807–9816

Acetylene Cyclotrimerization by Early Second-Row Transition Metals in the Gas Phase. A Theoretical Study

Mayra Martinez, Maria del Carmen Michelini, Ivan Rivalta, Nino Russo, and Emilia Sicilia*

Dipartimento di Chimica and Centro di Calcolo ad Alte Prestazioni per Elaborazioni Parallele e Distribuite-Centro d'Eccellenza MURST, Università della Calabria, I-87030 Arcavacata di Rende, Italy

Received July 29, 2005

The acetylene cyclotrimerization reaction mediated by the left-hand-side bare transition metal atoms Y, Zr, Nb, and Mo has been studied theoretically, employing DFT in its B3LYP formulation. The complete reaction mechanism has been analyzed, identifying intermediates and transition states. Both the ground spin state and at least one low-lying excited state have been considered to establish whether possible spin crossings between surfaces of different multiplicity can occur. Our results show that the overall reaction is highly favorable from a thermodynamic point of view and ground state transition states lie always below the energy limit represented by ground state reactants. After the activation of two acetylene molecules and formation of a bis-ligated complex, the reaction proceeds to give a metallacycle intermediate, as the alternative formation of a cyclobutadiene complex is energetically disfavored. All the examined reaction paths involve formation of a metallacycloheptatriene intermediate that in turn generates a metal–benzene adduct from which finally benzene is released. Similarities and differences in the behaviors of the considered four metal atoms have been examined.

1. Introduction

Transition metals are involved in a myriad of catalytic processes, and their all-pervading presence finds an explanation in their ability to adopt different oxidation states, coordination modes, bonding patterns, etc. One approach that has been revealed to be very precious for chemists in their attempt to better understand these systems was to study model reactions in the gas phase, unencumbered by the effects of ligands and solvent.[1−21] A combination of experimental and computational studies of the reactivities of metal atoms and clusters in the gas phase can enhance our understanding of the elementary processes occurring in real catalysts, which is essential for a rational catalyst design. Computational chemistry studies facilitate systematic investigation of reactivities across entire rows of bare transition

* To whom correspondence should be addressed. Tel: +39-0984-492048. Fax: +39-0984-492044. E-mail: siciliae@unical.it.

(1) Allison, J.; Freas, R. B.; Ridge, D. P. *J. Am. Chem. Soc*. **1979**, *101*, 1332.
(2) *Gas-Phase Inorganic Chemistry*; Russel, D. H., Ed.; Plenum: New York, 1989; p 412.
(3) Armentrout, P. B.; Beauchamp, J. L. *Acc. Chem*. Res. **1993**, *26*, 213.
(4) Armentrout, P. B. In *Selective Hydrocarbons Activation: Principles and Progress*; Davies, J. A., Watson, P. L., Greenberg, A., Liebman, J. F., Eds.; VCH: New York, 1990.
(5) Armentrout, P. B. *Annu. Rev. Phys. Chem*. **1990**, *41*, 313.
(6) Eller, K.; Schwarz, H. *Chem. Rev.* **1991**, *91*, 1121.
(7) (a) Weisshaar, J. C. *Adv. Chem. Phys.* **1992**, 82, 213. (b) Weisshaar, J. C. *Acc. Chem*. Res. **1993**, *26*, 213.
(8) Armentrout, P. B.; Kickel, B. L. In *Organometallic Ion Chemistry*; Freiser, B. S., Ed.; Kluwer: Dordrecht, 1996.
(9) Armentrout, P. B. in *Topics in Organometallic Chemistry*; Brown, J. M., Hofmann, P., Eds.; Springer-Verlag: Berlin, 1999.
(10) Crabtree, R. H. *The Organometallic Chemistry of the Transition Metals*, 2nd ed.; John Wiley and Sons: New York, 1994.
(11) Somorjai, G. A. *Introduction to Surface Chemistry and Catalysis*; John Wiley and Sons: New York, 1994.
(12) (a) Siegbahn, P. E. M.; Blomberg, M. R. A. In *Theoretical Aspects of Homogeneous Catalysis*; van Leeuwen, P. W. N. M., Morokuma, K., van Lenthe, J. H., Eds.; Kluwer Academic Publishers: Dordrecht, 1995; p 15−63. (b) Wittborn, A. M. C.; Costas, M.; Blomberg, M. R. A.; Siegbahn, P. E. M. *J. Chem. Phys.* **1997**, *107*, 4318. (c) Blomberg, M. R. A.; Siegbahn, P. E. M.; Svensson, M. *J. Am. Chem. Soc*. **1992**, *114*, 6095.
(13) Musaev, D. G.; Morokuma, K. *J. Chem. Phys.* **1994**, *101*, 10697.
(14) Irigoras, A.; Fowler, J. E.; Ugalde, J. M. *J. Phys. Chem*. **1998**, *102*, 293.
(15) Irigoras, A.; Fowler, J. E.; Ugalde, J. M. *J. Am. Chem. Soc*. **1999**, *121*, 574; 8549.
(16) Irigoras, A.; Elizalde, O.; Silanes, I.; Fowler, J. E.; Ugalde, J. M. *J. Am. Chem. Soc*. **2000**, *122*, 114.
(17) Russo, N.; Sicilia, E. *J. Am. Chem. Soc*. **2001**, *123*, 2588.
(18) Russo, N.; Sicilia, E. *J. Am. Chem. Soc*. **2002**, *124*, 1471.
(19) Michelini, M. C.; Russo, N.; Sicilia, E. *J. Phys. Chem*. **2002**, *106*, 8937.
(20) Michelini, M. C.; Russo, N.; Sicilia, E. *Inorg. Chem.* **2004**, *43*, 4944.
(21) Chiodo, S.; Kondakova, O.; Irigoras, A.; Michelini, M. C.; Russo, N.; Sicilia, E.; Ugalde, J. M. *J. Phys. Chem.* A **2004**, *108*, 1069.

10.1021/ic051281k CCC: $30.25
Published on Web 11/12/2005

metal atoms, and the consequent comparison of barrier heights and reaction energetics provides fundamental insight into how electronic configuration and orbital occupancy control transition metals catalytic activity.

In the framework of a more extended project aimed to unravel the elementary mechanisms of catalytic processes for the activation of prototypical bonds mediated by transition metal containing systems, we have undertaken a systematic theoretical study of the cyclotrimerization of acetylene mediated by second-row transition metal atoms.

Cycloaddition of unsaturated hydrocarbons is a useful kind of reaction for the synthesis of organic ring systems. Although these reactions are generally quite exothermic, they are usually hampered by high kinetic barriers as long as nonactivated hydrocarbons are involved. Thermal cyclotrimerization of acetylene to form benzene is particularly interesting from this point of view since, even if this transformation is extremely exothermic, of about 142 kcal/mol,[22] it takes place only at temperatures higher than 400 °C. The results of the theoretical calculations performed on cyclotrimerization of acetylene have evidenced that high temperatures are required to overcome a prohibitive activation barrier calculated to lie in the 60−80 kcal/mol regime.[23] Thus, the synthetic advantages this reaction possesses cannot be exploited unless catalysts are used. Since the first announcement of acetylene cyclotrimerization on Pd at low temperatures,[24−26] a lot of theoretical and experimental studies, covering many structural, mechanistic, and kinetic aspects, have appeared in the literature dealing with acetylene cyclotrimerization to give benzene catalyzed by transition metals from bare and supported atoms to crystals.[27−41] However, they essentially concern the reactivity of late transition metals, particularly those from group 8, while the possibility to use early transition metals as catalysts to increase the rate of the studied process and to allow the use of milder reaction conditions, has been less extensively explored.[42]

In this work, we present the results of a detailed theoretical investigation of the acetylene cyclotrimerization reaction mediated by naked transition metal atoms from the left-hand side of the 4d series, that is Y, Zr, Nb, and Mo. Density Functional Theory (DFT) has been applied to characterize all the minima and first-order saddle points and to present a complete mechanistic scheme of the reaction.

The study of the mechanism of benzene formation was carried out from the hypothesis that the reaction proceeds through the consecutive addition of acetylene molecules without C−C bond scission. The possible alternative steps that can occur after adsorption of a second acetylene molecule have been taken into account, as reported in Scheme 1. Indeed, the two acetylene molecules can isomerize to form a complex containing a metallacycle (MC_4H_4) or a cyclobutadiene molecule bonded to the metal $M-C_4H_4$, or the $M-(C_2H_2)_2$ complex can prefer to adsorb a third one. As a consequence, the three acetylene molecules can isomerize in a concerted way to lead directly to the benzene formation, or from one of the MC_4H_4 or $M-C_4H_4$ complexes, the corresponding $(C_2H_2)-MC_4H_4$ and $(C_2H_2)-M-C_4H_4$ ones are formed. Finally, once one or the other of these latter two complexes is formed, the reaction can pass through a new metallacycle reaction intermediate MC_6H_6 before the benzene formation, $M-C_6H_6$.

The mechanistic details of the reaction under examination have been studied in accordance with the two-state reactivity (TSR) paradigm,[43] whose central idea was introduced, at first, by Armentrout and co-workers.[44,45] Due to accessibility of the excited states of the considered atoms, the possibility of spin crossing between surfaces of different multiplicity cannot be excluded. Indeed, in the reactions under study, it has been shown the importance of the analysis of more than one spin state.

2. Computational Details

Geometry optimizations and frequency calculations for all the reactants, intermediates, products, and transition states were performed at the density functional level of theory, employing Becke's three-parameter hybrid functional[46] combined with the Lee, Yang, and Parr (LYP)[47] correlation functional, denoted as B3LYP within the Gaussian03/DFT pacakge.[48] The LANL2DZ effective core potential[49] has been used for the metal center. In LANL2DZ, the valence shell are explicitly represented using a double-ζ. The valence electrons considered for the transition metals are $4s^2\ 4p^6\ 4d^2\ 5s^1$ for Y, $4s^2\ 4p^6\ 4d^2\ 5s^2$ for Zr, $4s^2\ 4p^6\ 4d^4\ 5s^1$ for Nb, and

(22) Benson, S. W. *Thermochemical Kinetics*; Wiley: New York, 1968.
(23) (a) Houk, K. N.; Gandour, R. W.; Strozier, R. W.; Rondan, N. G.; Paquette, L. A.; *J. Am. Chem. Soc.* **1979**, *101*, 6797. (b) Bach, R. D.; Wolber, G. J.; Schlegel, H. B. *J. Am. Chem. Soc.* **1985**, *107*, 2837.
(24) Tysoe, W. T.; Nyberg, G. L.; Lambert, R. M. *J. Chem. Soc., Chem. Commun.* **1983**, 623.
(25) Sesselmann, W. S.; Woratschek, B.; Ertl, G.; Kuppers J.; Haberland, H. *Surf. Sci*. **1983**, *130*, 245.
(26) Gentle, T. M.; Muetterties, E. L. *J. Phys. Chem*. **1983**, *87*, 2469.
(27) Holmblad, P. M.; Rainer, D. R.; Goodman, D. W. *J. Phys. Chem. B* **1997**, *101*, 8883.
(28) Abdelrehim, I. M.; Pelhos, K.; Madey, T. E.; Eng, J.; Chen, J. G. *J. Mol. Catal. A* **1998**, *131*, 107.
(29) Rucker, T. G.; Logan, M. A.; Gentle, T. M.; Muetterties E. L.; Somorjai, G. A. *J. Phys. Chem.* **1986**, *90*, 2703.
(30) Patterson, C. H.; Lambert, R. M. *J. Am. Chem. Soc*. **1988**, *110*, 6871.
(31) Zhu, X.-Y.; White, J. M. *Surf. Sci.* **1989**, *214*, 240.
(32) Mate, C. M.; Kao, C.-T.; Bent, B. E.; Somorjai, G. A. *Surf. Sci*. **1988**, *197*, 183.
(33) Ormerod, R. M.; Lambert, R. M. *J. Phys. Chem.* **1992**, *96*, 8111.
(34) Ormerod, R. M.; Lambert, R. M.; Hoffmann, H.; Zaera, F.; Yao, J. M.; Saldin, D. K.; Wang, L. P.; Bennet, D. W.; Tysoe, W. T. *Surf. Sci*. **1993**, *295*, 277.
(35) Pacchioni, G.; Lambert, R. M. *Surf. Sci.* **1994**, *304*, 208.
(36) Hoffmann, H.; Zaera, F.; Ormerod, R. M.; Lambert, R. M.; Yao, J. M.; Saldin, D. K.; Wang, L. P.; Bennett, D. W.; Tysoe, W. T. *Surf. Sci*. **1992**, *268*, 1.
(37) Abbet, S.; Sanchez, A.; Heiz, U.; Schneider, W.-D.; Ferrari, A. M.; Pacchioni, G.; Rösch, N. *J. Am. Chem. Soc.* **2000**, *122*, 3453.
(38) Abbet, S.; Sanchez, A.; Heiz U.; Schneider, W. D. *J. Catal*. **2001**, *198*, 122.
(39) Ferrari, A. M.; Giordano, L.; Pacchioni, G.; Abbet, S.; Heiz, U. *J. Phys. Chem. B* **2002**, *106*, 3173.
(40) Judai, K.; Wörz, A. S.; Abbet, S.; Antonietti, J. M.; Heiz, U. Del Vitto, A.; Giordano, L.; Pacchioni, G. *Phys. Chem. Chem. Phys.* **2005**, *7*, 955.
(41) Chrétien, S.; Salahub, D. R. *J. Chem. Phys.* **2003**, *119*, 12291.
(42) Buckner, S. W.; MacMahon, T. J.; Byrd, G. D.; Freiser, B. S. *Inorg. Chem.* **1989**, *28*, 3511.
(43) Schröder, D.; Shaik, S.; Schwarz, H. *Acc. Chem. Res.* **2000**, *33*, 139.
(44) Armentrout, P. B.; Beauchamp, J. L. *Acc. Chem. Res*. **1989**, *22*, 315.
(45) Armentrout, P. B. *Science* **1991**, *251*, 175.
(46) Becke, A. D. *J. Chem. Phys.* **1993**, *98*, 5648.
(47) Stephens, P. J.; Devlin, F. J.; Chabalowski, C. F.; Frisch M. J. *J. Phys. Chem*. **1994**, *98*, 11623.

Scheme 1

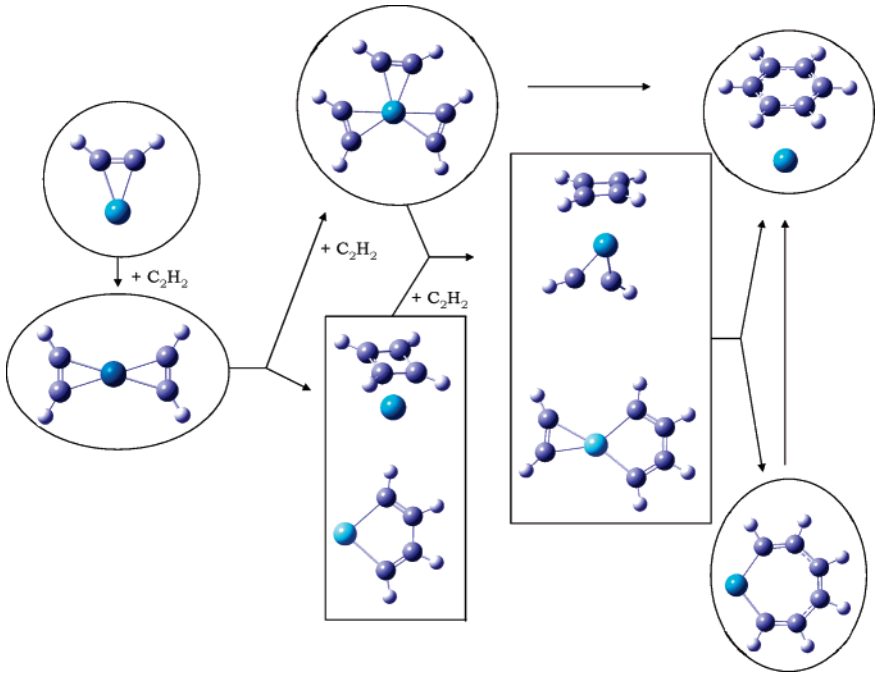

$4s^2$ $4p^6$ $4d^5$ $5s^1$ for Mo. The standard 6-311+G** basis set[50] has been employed for the rest of the atoms. Preliminary calculations performed adding polarization functions to the valence shell of the metal atom showed that the conclusions drown on the basis of the pathways reported in the present work are in no way qualitatively affected and the introduced changes in relative energies are less than 4 kcal/mol.

No symmetry restrictions were imposed during the geometry optimizations, whereas for each optimized stationary point, vibrational analysis was performed to determine its character (minimum or saddle point) and to evaluate the zero-point vibrational energy (ZPVE) corrections, which are included in all relative energies. For all the reported transition states, it has been carefully checked that the vibrational mode associated to the imaginary frequency corresponds to the correct movement of involved atoms. All the minima connected by a given transition state were confirmed by intrinsic reaction coordinate (IRC)[51] driving calculations (in mass-weighted corordinates) as implemented in the Gaussian03 program.

The counterpoise corrections have been calculated to correct binding energies (BE) for basis set superposition error (BSSE).[52] The introduced corrections for some of the considered complexes significantly change the noncorrected values.

For all the studied species, we have checked $\langle S^2 \rangle$ values to evaluate whether spin contamination can influence the quality of the results. In all cases, we have found that the calculated values differ from $S(S + 1)$ by less that 5%.

A full natural bond orbital (NBO) analysis[53,54] has been performed for all the stationary points along the energy paths to give further insight into their bonding properties.

3. Results and Discussion

In our investigation for benzene formation from acetylene mediated by early bare second-row transition metals according to the sequence of steps proposed into the schematic representation of the mechanism (see Scheme 1), the formation of all the possible complexes has been taken into consideration. For all the metals involved in this study, the cyclotrimerization process invariably takes place via the following steps: (a) coordination and activation of an acetylene molecule; (b) coordination and activation of a second acetylene molecule to form a $M-(C_2H_2)_2$ complex; (c) formation of a metallacycle, MC_4H_4, complex that implies overcoming a barrier for the first transition state of the reaction; (d) coordination and activation of a third acetylene molecule to form a $(C_2H_2)-MC_4H_4$ complex; (e) formation of a MC_6H_6 metallacycle intermediate that again implies overcoming an energy barrier for the second transition state along the reaction path; and (f) formation of a final complex corresponding to benzene formation through a third transition state followed by benzene elimination

(48) Frisch, M. J.; Trucks, G. W.; Schlegel, H. B.; Scuseria, G. E.; Robb, M. A.; Cheeseman, J. R.; Montgomery, J. A., Jr.; Vreven, T.; Kudin, K. N.; Burant, J. C.; Millam, J. M.; Iyengar, S. S.; Tomasi, J.; Barone, V.; Mennucci, B.; Cossi, M.; Scalmani, G.; Rega, N.; Petersson, G. A.; Nakatsuji, H.; Hada, M.; Ehara, M.; Toyota, K.; Fukuda, R.; Hasegawa, J.; Ishida, M.; Nakajima, T.; Honda, Y.; Kitao, O.; Nakai, H.; Klene, M.; Li, X.; Knox, J. E.; Hratchian, H. P.; Cross, J. B.; Bakken, V.; Adamo, C.; Jaramillo, J.; Gomperts, R.; Stratmann, R. E.; Yazyev, O.; Austin, A. J.; Cammi, R.; Pomelli, C.; Ochterski, J. W.; Ayala, P. Y.; Morokuma, K.; Voth, G. A.; Salvador, P.; Dannenberg, J. J.; Zakrzewski, V. G.; Dapprich, S.; Daniels, A. D.; Strain, M. C.; Farkas, O.; Malick, D. K.; Rabuck, A. D.; Raghavachari, K.; Foresman, J. B.; Ortiz, J. V.; Cui, Q.; Baboul, A. G.; Clifford, S.; Cioslowski, J.; Stefanov, B. B.; Liu, G.; Liashenko, A.; Piskorz, P.; Komaromi, I.; Martin, R. L.; Fox, D. J.; Keith, T.; Al-Laham, M. A.; Peng, C. Y.; Nanayakkara, A.; Challacombe, M.; Gill, P. M. W.; Johnson, B.; Chen, W.; Wong, M. W.; Gonzalez, C.; Pople, J. A. *Gaussian 03*, revision A.1; Gaussian, Inc.: Wallingford, CT, 2004.
(49) (a) Hay, P. J.; Wadt, W. R. *J. Chem. Phys.* **1985**, *82*, 270. (b) Hay, P. J.; Wadt, W. R. *J. Chem. Phys.* **1985**, *82*, 284. (c) Hay, P. J.; Wadt, W. R. *J. Chem. Phys.* **1985**, *82*, 299.
(50) (a) Krishnan, R.; Binkley, J. S.; Seeger, R.; Pople, J. A. *J. Chem. Phys.* **1980**, *72*, 650. (b) Blaudeau, J. P.; McGrath, M. P.; Curtis, L. A.; Radom, L. *J. Chem. Phys.* **1997**, *107*, 5016.
(51) (a) Gonzales, C.; Schlegel, H. B. *J. Chem. Phys.* **1989**, *90*, 2154. (b) Gonzales, C.; Schlegel, H. B. *J. Phys. Chem.* **1990**, *94*, 5523.
(52) Boys, S. B.; Bernardi, F. *Mol. Phys.* **1970**, *19*, 553.
(53) Carpenter, J. E.; Weinhold, F. *J. Mol Struct. (THEOCHEM)* **1988**, *169*, 41.
(54) Carpenter, J. E.; Weinhold, F. J. *The Structure of Small Molecules and Ions*; Plenum: New York, 1988.

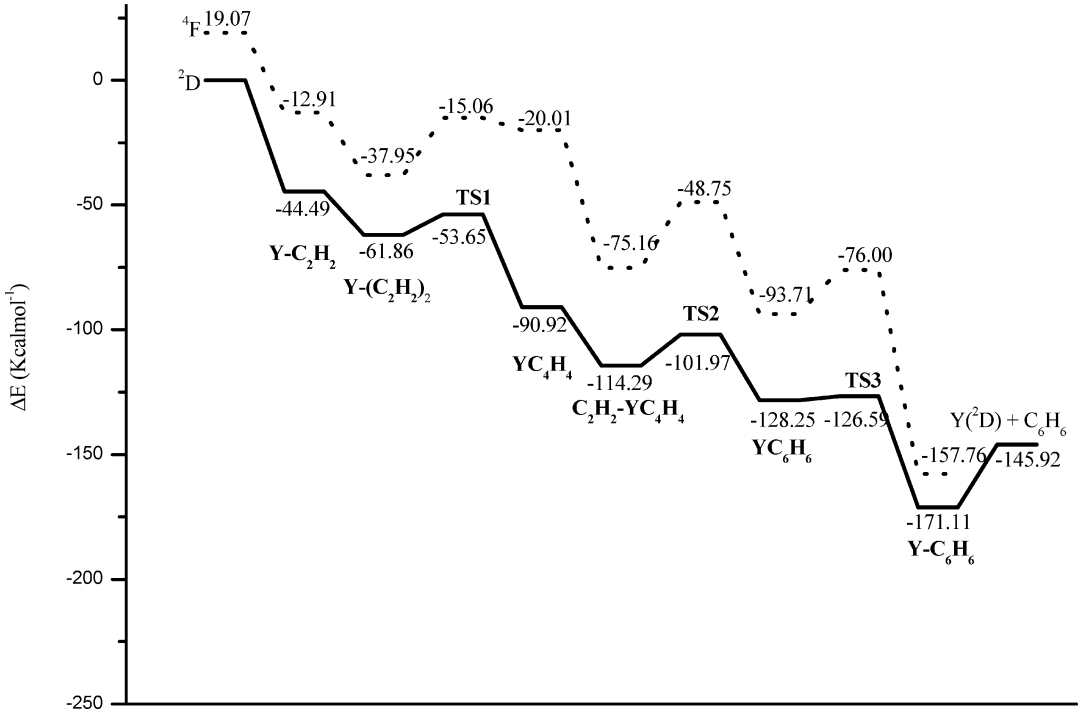

Figure 1. Doublet and quartet potential energy surfaces for the reaction $Y + 3C_2H_2$. Energies are in kcal/mol and relative to the ground-state reactants.

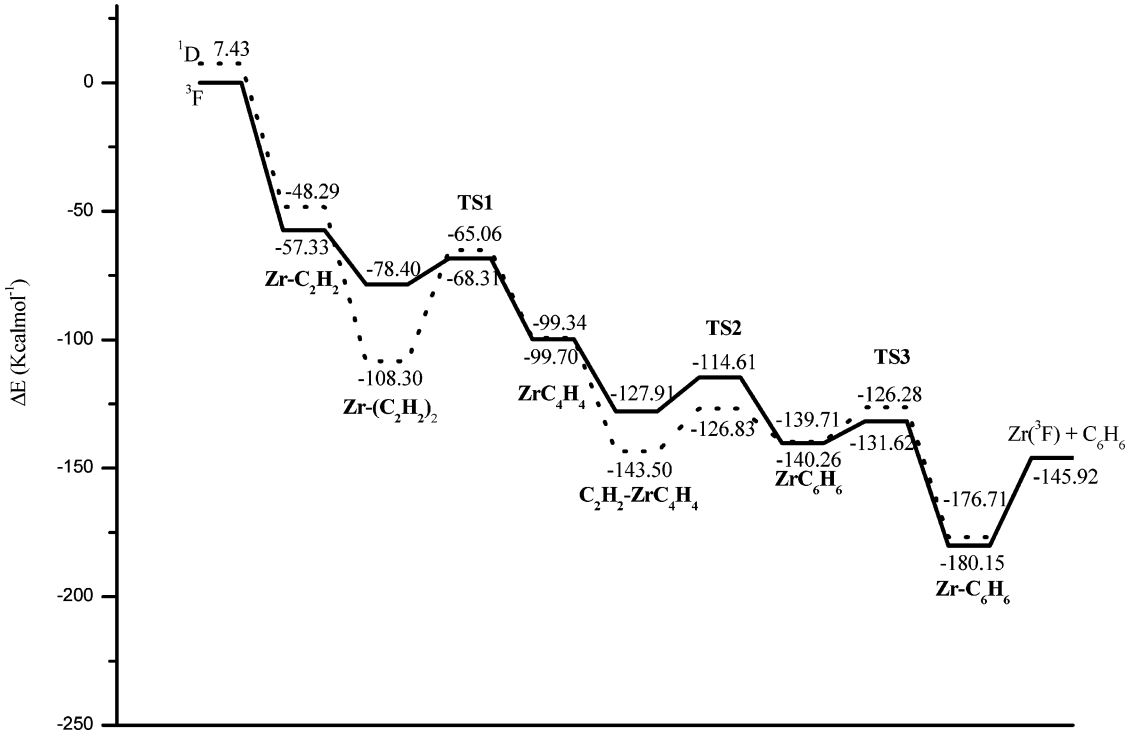

Figure 2. Triplet and singlet potential energy surfaces for the reaction $Zr + 3C_2H_2$. Energies are in kcal/mol and relative to the ground-state reactants.

The possibility that the reaction goes through the formation of a cyclobutadiene, $M-C_4H_4$, complex was ruled out since this intermediate for all the considered metals lies higher in energy with respect to the corresponding metallacycle complex. In the same way, any attempt to follow the pathway that from three acetylene molecules leads directly to benzene formation through a concerted mechanism was unsuccessful. On the other hand, it is noteworthy that a metallacycle, MC_6H_6, intermediate was always localized along the reaction pathways before benzene formation.

The occurrence of possible spin crossing between surfaces of different spin multiplicity has been highlighted along all the considered pathways, except for yttrium. However, to establish whether spin multiplicity has to be considered an additional factor in determining reactivity, more detailed investigations are needed and further work, involving the

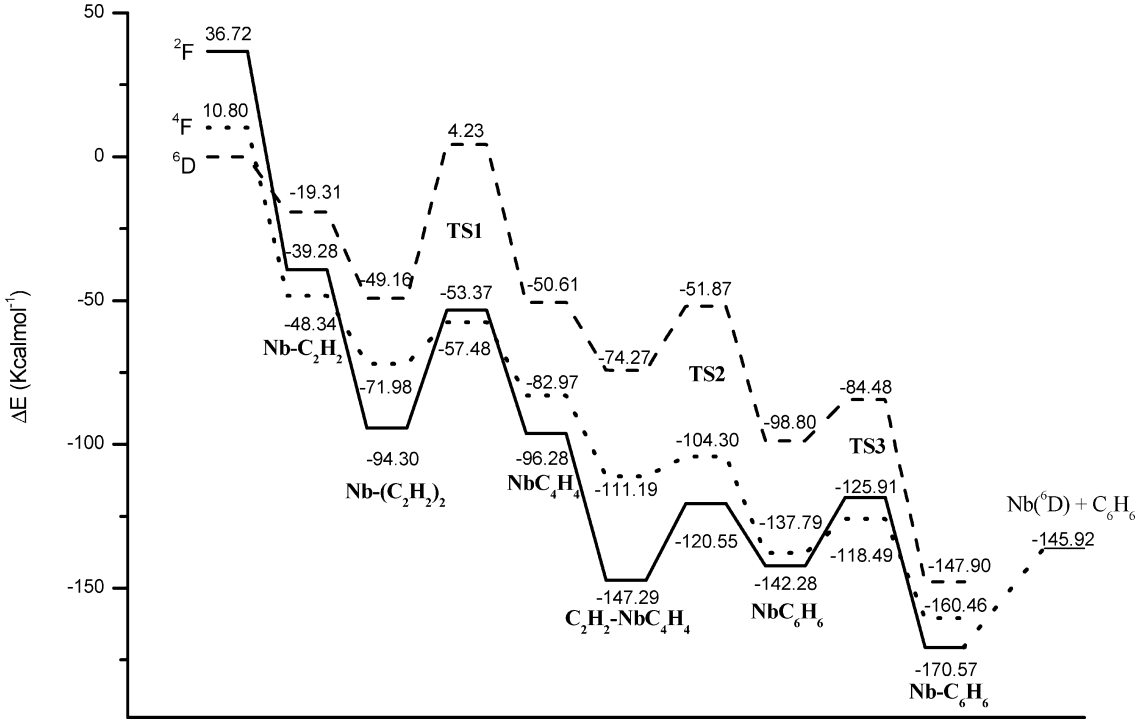

Figure 3. Sextet, quartet, and doublet potential energy surfaces for the reaction Nb + $3C_2H_2$. Energies are in kcal/mol and relative to the ground-state reactants.

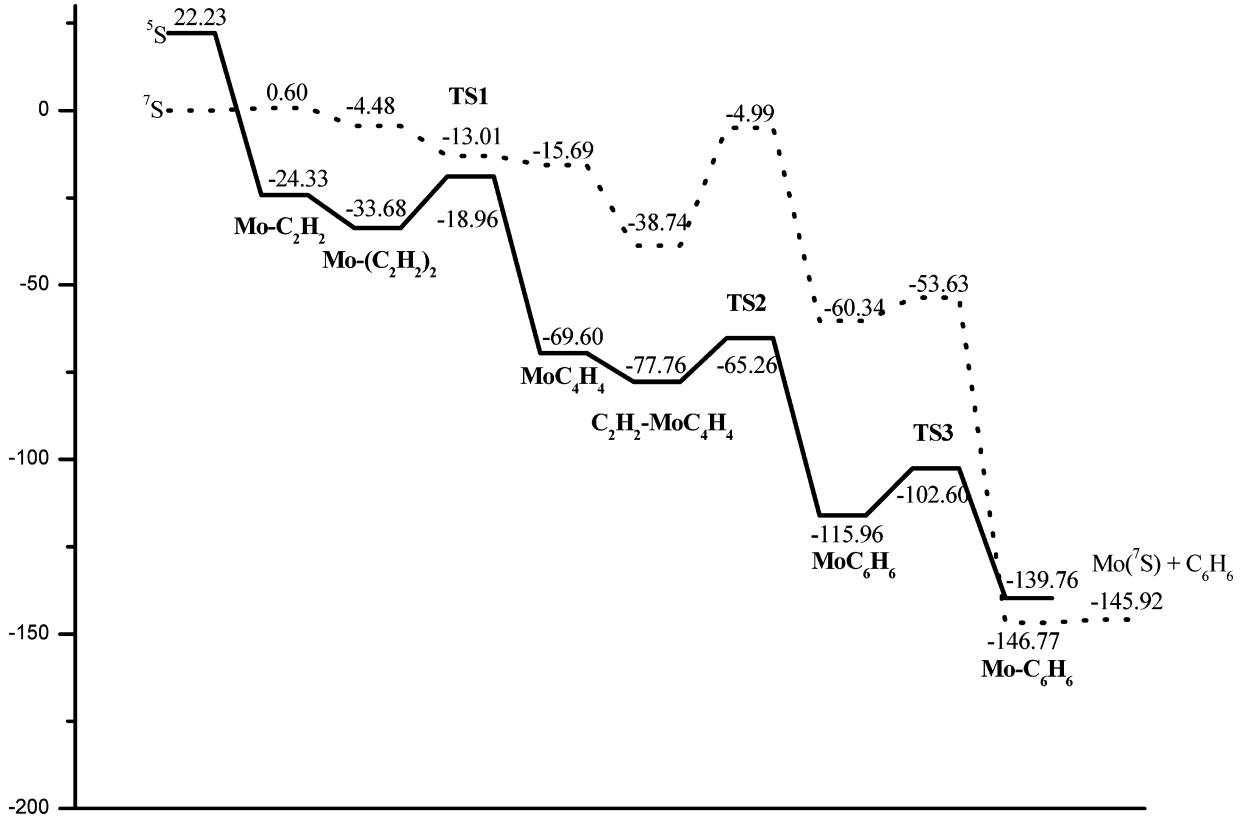

Figure 4. Sextet and quintet potential energy surfaces for the reaction Mo + $3C_2H_2$. Energies are in kcal/mol and relative to the ground-state reactants.

use of appropriate computational tools, will be devoted to this aim.

The potential energy surfaces for the complete cyclotrimerization of acetylene to give benzene are reported in Figures 1, 2, 3, and 4 for Y, Zr, Nb, and Mo, respectively. Relative energies are reported with respect to the reactant's limit represented by the isolated metal atom in its ground state and three acetylene molecules and have been corrected for ZPE but not for BSSE to allow a fair comparison between minima and transition states. In Tables 2−5 are reported the

Scheme 2

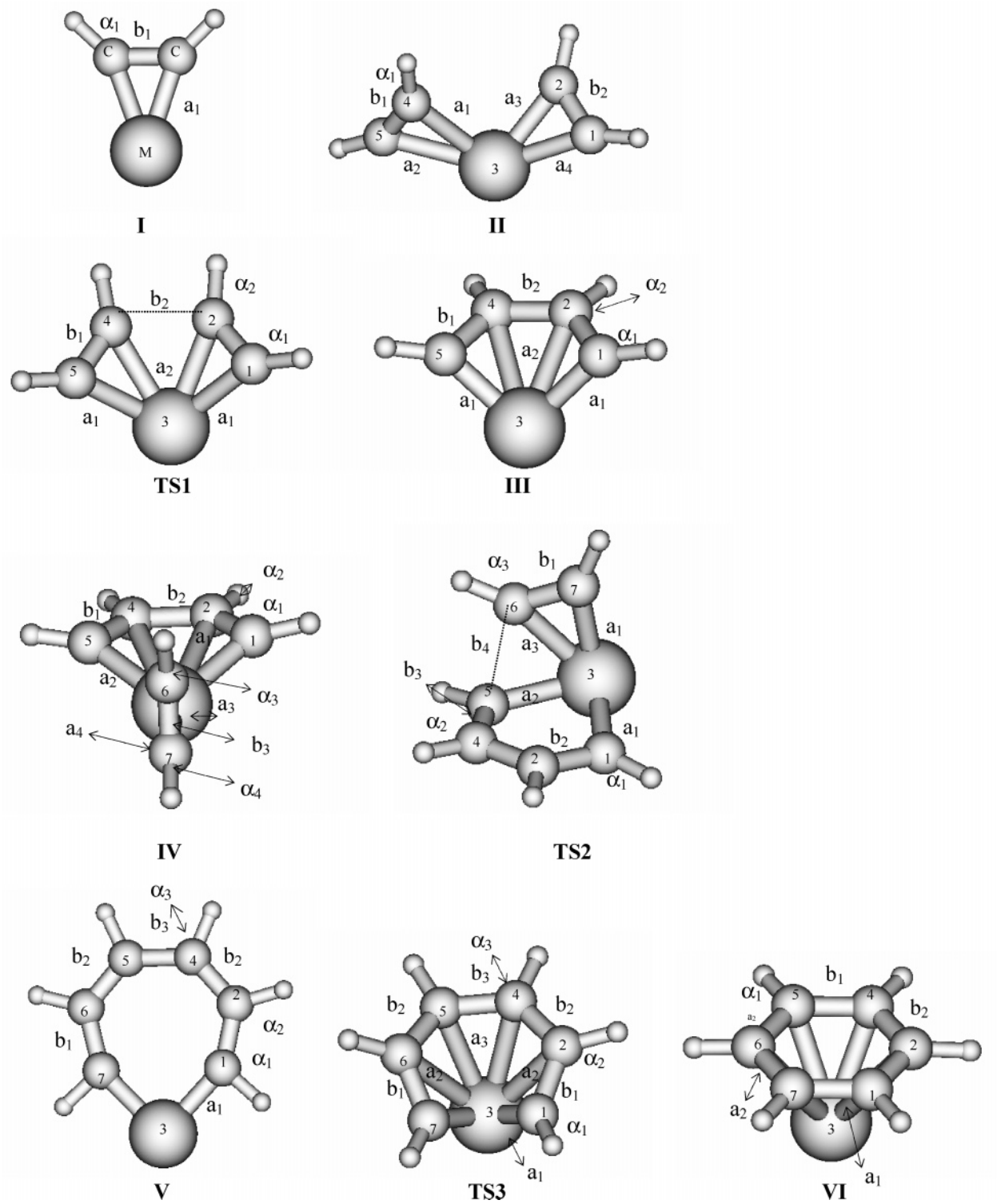

most relevant geometrical parameters for the ground-state minima and transition states according to the notation adopted in Scheme 2. In Table 6 are collected binding energies for $M-C_2H_2$, $M-(C_2H_2)_2$, and $C_2H_2-MC_4H_4$ complexes corrected for BSSE to show as this correction can be significant for some of them.

3.1. Excitation Energies. To evidence the possibility of spin crossing between PESs of different multiplicity in all the studied reactions, at least two different spin states have been taken into account, and in the case of Nb, it was necessary to investigate three different spin states. Therefore, we first analyze the calculated energy splitting between the ground spin state and the excited state of interest for the bare metal atoms. In Table 1 are reported the energy gaps of the indicated excited state with respect to the ground spin state of the bare metals, which are Y (^{2}D, [Kr] 4d 5s^2), Zr (^{3}F, [Kr] 4d^2 5s^2), Nb (^{6}D, [Kr] 4d^4 5s), and Mo (^{7}S, [Kr] 4d^5 5s).

Table 1. Relative Energies (kcal/mol) for the First Excited States of the Bare Metal Atoms with Respect to the Corresponding Ground States

atom	state	this work	exptl[a]
Y	^{2}D (ds^2)	0.0	0.0
	4F (d^2s)	19.1	31.5
Zr	^{3}F (d^2s^2)	0.0	0.0
	1D (d^2s^2)	7.4	12.6
Nb	^{6}D (d^4s)	0.0	0.0
	4F (d^3s^2)	11.1	4.3
	^{2}G (d^3s^2)	36.7	24.3
Mo	^{7}S (d^5s)	0.0	0.0
	5S (d^5s)	22.2	30.8

[a] Reference 55.

As can be seen, at B3LYP/LANL2DZ level of theory, the energetic ordering of the states is correctly predicted in all cases even if the experimental gaps[55] are in almost all cases underestimated. The only exception is represented by Nb for which the ^{4}F $-^6$D gap is overestimated by 6.8 kcal/mol and the main deviation has been found for its second excited-state whose energy is overestimated by 12.4 kcal/mol with respect to the experimental value.

3.2. Coordination and Activation of One and Two Acetylene Molecules. The interaction between a transition metal and acetylene can be described by the Chatt−Dewar−Duncanson (CDD) mechanism[56] in which acetylene donates parts of the π electrons to an empty σ orbital of the metal. As a consequence, the π bond of acetylene is weakened and the π^* orbital is lowered in energy so that electrons can be accepted from a back-donating d orbital of the metal atom. This description of the binding mechanism is very general and at least three different situations, which can be preferred by different transition metals, can be characterized. Indeed, the back-bonding donating d orbital can be initially singly or doubly occupied or normal covalent bonds can be formed. Covalent bond formation, indeed, can be considered as an extreme of the donation bonding and leads to formation of a metallacyclopropene complex, so-called because the triple bond is broken and two covalent bonds are formed between the metal and the two carbon atoms in a three-member ring.[57] Previous theoretical studies have evidenced that the bonding of acetylene complexes for cations to the left side of the transition metal second row is characterized as normal covalent bonding forming metallacyclic compounds as the metal ion inserts into the in-plane π bond of acetylene.[58] The results of our investigation confirm this trend for the complexes formed with the corresponding neutrals. The definitive breaking of the π bond of the first acetylene molecule can be monitored both by the elongation of the C−C bond and the distortion of the bond angle H−C−C (see Tables 2−5) with respect to the gas-phase values (calculated d(C−C)=1.206 Å), as well as by the short C−M bond distances. NBO analysis clearly shows the existence of a double C−C and two C−M covalent bonds. Computed binding energies are 44.49 kcal/mol for Y, 57.33 kcal/mol for Zr, 48.34 kcal/mol for Nb, and 24.33 kcal/mol for Mo. The calculated values appear to be not proportional to the perturbation of the acetylene geometry since the promotion energy to the appropriate binding $4d^{n+1}5s$ state and the loss of exchange energy act differently in going from Y to Mo. The ground state of the complex corresponds to the ground state of the bare metal atom for Y and Zr, while for Nb and Mo, the complex ground state corresponds to the first low-spin excited state of the bare atom. This means that a spin crossing at the entrance channel occurs for both Nb and Mo (see Figures 3 and 4).

Coordination of a second acetylene molecule occurs with an energy release comparable to that for the first one only for Zr and Nb, while for Y and Mo, the strength of the bond significantly decreases. Indeed, binding energies, calculated as $E[M(C_2H_2)_2] - E[(M(C_2H_2)] - E(C_2H_2)$, are 17.47, 50.97, 45.96, and 9.35 kcal/mol for Y, Zr, Nb, and Mo, respectively. The extent of the coordination depends again on the donation and back-donation mechanism and can be measured by the gas-phase geometry distortion of the acetylene molecule (see Tables 2−5). The C−C bond of the second acetylene molecule appears to be elongated to a lesser extent with respect to the first one for Y. In the same way, the M−C distance is longer and the acetylenic C−C−H angle is less distorted from linearity. The C−C bond lengths for the two activated acetylene molecules in the Zr and Nb complexes are the same and are significantly longer than those in the free molecule, while for Mo, the complex is characterized by two C−C bond distances again equal among them but less significantly elongated with respect the bare C_2H_2. NBO analysis confirms again the preference for a back-bonding interaction leading to metallacycles for the bisacetylene complexes of Zr and Nb. A mixed back-donating mechanism is shown to exist in the case of Y and Mo for the coordination of the second acetylene molecule as the formation of a partial covalent bond occurs together with back-donation into the acetylene π^* orbital. The main difference between Y and Mo concerns, as expected, the amount of electron density transferred to the antibonding orbital. Indeed, in-plane π^* NBO population is very low, 0.037e, for the Y complex, whereas a large population of 0.201e is found in the case of Mo. As is shown in Tables 2−5, the two acetylene molecules are nearly parallel to each other in the Y and Zr complexes and form C−M−C angles of 116.3° and 99.6°, respectively. The Nb complex is slightly distorted from planarity, and the bisacetylene complex is perfectly planar in the case of Mo. In all cases, the coordination of the second acetylene molecule generates complexes whose ground states correspond to the lowest spin state of the bare metal atom, independently of the ground spin state of the bare atom. This means a doublet, singlet, doublet, and quintet ground state for the complexes of Y, Zr, Nb, and Mo, respectively, and therefore, a spin crossing occurs for Zr and Nb.

3.3. MC_4H_4 Intermediate Formation. So far, the considered processes of acetylene coordination are not activated, whereas the oxidative coupling of acetylene to form a MC_4H_4 complex implies to surmount the first energy barrier for the process. The process involves the formation of a new σ bond

(55) Moore, C. E. *Atomic Energy Levels*; NSRD-NBS, U.S. Government Printing Office: Washington, DC, 1991; Vol 1.
(56) (a) Dewar, M. J. S. *Bull. Soc. Chim. Fr.* **1951**, 79. (b) Chatt, J.; Duncanson, L. A. *J. Chem. Soc.* **1953**, 2939.
(57) Frenking, G.; Fröhlich, N. *Chem. Rev.* **2000**, *100*, 717.
(58) Sodupe, M.; Bauschlicher, C. W. *J. Phys. Chem.* **1991**, *95*, 8640.

Table 2. Selected Bond Lengths (Å) and Angles (deg) Corresponding to the Ground Spin States of All the Stationary Points Involved in the Reaction Y + 3 C_2H_2 (See Scheme 2).

structure − state[a]	a_1, a_2, a_3, a_4	b_1, b_2, b_3, b_4	$\alpha_1, \alpha_2, \alpha_3, \alpha_4$	$\beta_1, \beta_2, \beta_3$
I − $^2A'$	2.211	1.347	127.4	−
II − ^2A	2.240, 2.240, 2.467	1.346, 1.274	126.3, 126.3, 142.7	117.2, 84.1
TS1 − ^2A	2.337, 2.473, 2.275	1.236, 2.724	132.4, 134.0	179.7, 179.6
III − $^2B_1$	2.923, 2.299	1.358, 1.489	116.8, 121.0	180.0, 180.0
IV − ^2A	2.848, 2.313, 2.518, 2.492	1.363, 1.500, 1.267	115.4, 120.1, 144.7, 144.6	179.1, 178.5, −90.4
TS2 − ^2A	2.336, 2.275, 2.511	1.389, 1.369, 1.287, 2.392	115.9, 120.5, 138.1	−179.0, −178.1, 33.0
V − ^2A	2.292	1.359, 1.458, 1.366	114.8, 119.7, 113.8	36.7, 0.1, 0.1[b]
TS3 − ^2A	2.255, 2.804, 2.863	1.379, 1.432, 1.400	118.1, 120.6, 115.7	32.3, 0.2, 0.1[b]
VI − ^2A	2.416, 2.643	1.368, 1.461	119.5	−24.9, 0.0, 0.0[b]

[a] Ground spin state structure. As indicated in Scheme 2 a_i, distance M−C; b_i, C−C distances as indicated in Figure 1; α_i, C−C−H angles as indicated in Scheme 2; β_i, selected dihedral angles (β_1: $_{1234}$, β_2: $_{1235}$, β_3: $_{2467}$, following the numeration indicated in Scheme 2. [b] β_1: $_{1245}$, β_2: $_{2456}$, β_3: $_{1267}$.

Table 3. Selected Bond Lengths (Å) and Angles (deg) Corresponding to the Ground Spin States of All the Stationary Points Involved in the Reaction Zr + 3 C_2H_2 (See Figures 1 and 3)

structure − state[a]	a_1, a_2, a_3, a_4	b_1, b_2, b_3, b_4	$\alpha_1, \alpha_2, \alpha_3, \alpha_4$	$\beta_1, \beta_2, \beta_3$
I − $^3A_2$	2.096	1.344	132.1	−
II − ^1A	2.141, 2.141, 2.141	1.333, 1.333	131.6, 131.6	112.8, 77.0
TS1 − ^3A	2.284, 2.212, 2.212	1.301, 2.078	132.4, 139.3	−151.0, −166.6
III − $^3B_1$	2.837, 2.161, 2.141	1.378, 1.453	117.9, 120.9	180.0, 180.0
IV − ^1A	2.201, 2.201, 2.141, 2.164	1.364, 1.506, 1.333	117.4, 120.1, 128.9, 132.3	−179.9, −179.3, −85.7
TS2 − ^1A	2.113, 2.184, 2.235	1.415, 1.400, 1.337, 1.994	117.6, 120.9, 132.8	168.7, 163.2, −4.6
V − ^3A	2.132	1.388, 1.446, 1.433	120.6, 120.6, 112.6	23.5, −0.2, 0.0[b]
TS3 − ^3A	2.112, 2.514, 2.518	1.404, 1.416, 1.422	123.9, 120.8, 116.0	22.3, 8.5, −3.7[b]
VI − ^3A	2.300, 2.402	1.401, 1.451	120.2	0.2, −13.8, −7.0 [b]

[a] Ground spin state structure. As indicated in Scheme 2 a_i, distance M−C; b_i, C−C distances as indicated in Figure 1; α_i, C−C−H angles as indicated in Figure 1; β_i, selected dihedral angles (β_1: $_{1234}$, β_2: $_{1235}$, β_3: $_{2467}$, following the numeration indicated in Scheme 2. [b] β_1: $_{1245}$, β_2: $_{2456}$, β_3: $_{1267}$

Table 4. Selected Bond Lengths (Å) and Angles (deg) Corresponding to the Ground Spin States of All the Stationary Points Involved in the Reaction Nb + 3 C_2H_2

structure − state[b]	a_1, a_2, a_3, a_4	b_1, b_2, b_3, b_4	$\alpha_1, \alpha_2, \alpha_3, \alpha_4$	$\beta_1, \beta_2, \beta_3$
I − $^4A''$	2.048	1.333	136.2	−
II − ^2A	2.046, 2.135, 2.142	1.336	128.2, 137.2	140.6, 171.2
TS1 − $^4A''$	2.228, 2.135	1.312, 1.972	131.5, 138.0	147.9, 130.0
III − ^2A	2.326, 1.969	1.420, 1.433	123.7, 121.5	146.8, 126.9
IV − ^2A	2.538, 2.055, 2.087, 2.107	1.387, 1.462, 1.315	121.1, 121.2, 139.6,134.9	158.8, 146.3, 92.1
TS2 − ^2A	2.061, 2.119, 2.185	1.418,1.405, 1.321, 2.015	118.1, 121.5, 136.9	167.6, 161.7, 176.8
V − ^2A	1.915	1.410, 1.379, 1.425	120.1, 117.4, 114,1	0.0, 0.0, 0.0[b]
TS3 − ^2A	2.010, 2.502, 2.370	1.390, 1.410, 1.436	126.9, 122.6, 115.8	19.7, 12.1, 4.6[b]
VI − ^2A	2.245	1.439	120.0	0.0, 0.0, 0.0[b]

[a] Ground spin state structure. As indicated in Scheme 2 a_i, distance M−C; b_i, C−C distances as indicated in Figure 1; α_i, C−C−H angles as indicated in Figure 1; β_i, selected dihedral angles (β_1: $_{1234}$, β_2: $_{1235}$, β_3: $_{2467}$, following the numeration indicated in Scheme 2. [b] β_1: $_{1245}$, β_2: $_{2456}$, β_3: $_{1267}$

Table 5. Selected Bond Lengths (Å) and Angles (deg) Corresponding to the Ground Spin States of All the Stationary Points Involved in the Reaction Mo + 3C_2H_2

structure − state[1]	a_1, a_2, a_3	b_1, b_2, b_3, b_4	$\alpha_1, \alpha_2, \alpha_3$	$\beta_1, \beta_2, \beta_3$
I − $^5B_2$	2.069	1.305	140.3	−
II − ^5A	2.204, 2.217, 2.217	1.265, 1.265	146.5, 150.0	180.0, −180.0
TS1 − ^5A	2.255, 2.143, 2.143	1.304, 1.989	128.9, 138.0	−158.2, −170.3
III − ^5A	2.862, 2.106, 2.106	1.354, 1.476	120.8, 122.4	179.9, 179.9
IV − ^5A	2.902, 2.159, 2.536	1.356, 1.474, 1.217	121.1, 122.5,170.0	180.0, 180.0, −86.8
TS2 − ^5A	2.155, 2.090, 2.598	1.381, 1.362, 1.271, 2.411	120.1, 122.3, 155.9	176.6, 177.3, 26.0
V − ^5A	2.039	1.363, 1.447, 1.367	115.6, 116.3, 112.9	−0.1, 0.0, 0.0[b]
TS3 − ^5A	2.075, 3.050, 3.050	1.380, 1.418, 1.386	117.6, 118.3, 117.2	27.0, 0.0, 0.0[b]
VI − ^2A	4.032	1.392	120.0	0.0, 0.0, 0.0[b]

[a] Ground spin state structure. As indicated in Scheme 2 a_i, distance M−C; b_i, C−C distances as indicated in Figure 1; α_i, C−C−H angles as indicated in Figure 1; β_i, selected dihedral angles (β_1: $_{1234}$, β_2: $_{1235}$, β_3: $_{2467}$, following the numeration indicated in Scheme 2. [b] β_1: $_{1245}$, β_2: $_{2456}$, β_3: $_{1267}$

between two C atoms of adjacent acetylene molecules and eventually of new σ M−C bonds at the expenses of π interactions in the M−$(C_2H_2)_2$ complexes. The overall energetic balance due to bonding changes occurring during this transformation gives the following results: the formation of the MC_4H_4 metallacycle intermediate is highly exothermic with respect to separated reactants (M + $2C_2H_2$) in all the neutral metal atoms considered here, but the MC_4H_4 species is more stable than the complex with two adsorbed acetylene molecules only for Y and Mo by 51.94 and 35.92 kcal/mol, respectively. The same conversion from M−$(C_2H_2)_2$ to MC_4H_4 is endothermic for Zr and thermoneutral for Nb. At a first glance from the geometrical parameters reported in Tables 2−5 appears evident the formation of a new σ bond

Table 6. Binding Energies Corrected for BSSE (Reported in Parentheses) for the Minima Corresponding to the Activation of One, Two, and Three Acetylene Molecules along the Pathway for the Cyclotrimerization Reaction

metal	$M-C_2H_2$	$M-(C_2H_2)_2$	$C_2H_2-MC_4H_4$
Y	42.02 (3.37)	13.54 (3.93)	18.83 (4.54)
Zr	52.24 (5.09)	48.53 (2.44)	40.45 (3.35)
Nb	47.18 (1.16)	44.07 (1.89)	48.92 (2.09)
Mo	22.93 (1.40)	7.63 (1.72)	6.32 (2.04)

between C atoms and the definitive elongation of the intramolecular C−C distances. However, for Nb, the formed complex is not planar, the C−C distances are almost equal among them, and the new C−C bond is almost formed but the two corresponding Nb−C bonds are not completely broken yet.

Location of the transition states for the conversion process reveals a low energy barrier, of 8.21 kcal/mol, for Y. The same barrier becomes 40.0 kcal/mol for Zr, 36.82 kcal/mol for Nb, and 14.72 kcal/mol for Mo. This trend implies a transition-state structure quite geometrically similar to the reactant in the first case and dissimilar in the other cases, as is confirmed by the structural parameters reported in Tables 2−5, and particularly the intermolecular C−C distance (2.724 Å) that is very long yet for yttrium transition state. All the transition state structures localized along the PESs lie below the separate reactants dissociation limit, and since for Zr and Nb the ground-state multiplicity changes, spin crossings are involved even if ground spin state of reactant $M(C_2H_2)_2$ and product MC_4H_4 is the same.

3.4. Coordination of a Third Acetylene Molecule. Coordination of a third acetylene molecule to the metallacyclopentadiene complex represents a key step in the process toward benzene formation since it involves the metal's ability to activate another acetylene molecule. Previous calculations showed that an unsupported Pd atom is unable to add and activate three acetylene molecules,[59] and the step appears to be critical also in the case of transition metal complexes.[60] The bare metal atoms considered here show different behaviors. The activation of the third acetylene molecule is monitored again by the distortion of the geometrical parameters of the bonded molecule with respect to the gas-phase values. A considerable back-bonding interaction results in the elongation of the C−C bond and a reduction of the acetylenic C−C−H angle for both Zr and Nb, and the energy of the additional interaction amounts to 43.80 and 51.01 kcal/mol, respectively. The framework of the metallacyclopentadiene complex is slightly perturbed: both the long C−C and the M−C bonds are longer than those found in **III**.

The Y atom is also able to coordinate and activate the third acetylene molecule even if the interaction is less strong, the process being exothermic by 23.37 kcal/mol, and the same behavior is observed concerning a slight lengthening of the metallacycle bonds and a significant distortion of the bond distance and angles of the activated molecule (see Table 2). Also in this case, the NBO analysis shows a mixed back-bonding interaction, which involves formation of partial covalent bonds and contemporary electron density transfer to the acetylene π^* orbital. In contrast, the third C_2H_2 molecule is weakly bound to the MoC_4H_4 intermediate (by only 8.36 kcal/mol), without an appreciable activation of the molecule; indeed, the C−C distance is 1.217 Å and the H−C−C bond angle is 170.0°, Table 4. However, the formed adduct is stable enough and does not show any tendency to dissociate.

Since the coordination of the third acetylene can occur to give either of two conformations with the acetylene molecule situated perpendicular or parallel to the plane containing the cycle, both structures were optimized for all the considered metals. The obtained results indicate a distinct energetic preference for the perpendicular orientation over the parallel one resulting primarily from symmetry requirements of the orbitals involved into the formation of bonds.

3.5. MC_6H_6 Intermediate Formation. After the activation of the third acetylene, two mechanisms for benzene formation appear conceivable, that is, the direct intermolecular cycloaddition of the coordinated acetylene to the MC_4H_4 intermediate or the insertion of the alkyne in the metal−carbon σ bond of the metallacyclopentadiene to form a new metallacycle intermediate, **V**. Although previous theoretical works on the same subject unfavorably considered the second route toward benzene formation,[39,59,60] for the cases examined here, any attempt to obtain benzene directly from intermediate **IV** were unsuccessful, and stable metallacycles, MC_6H_6, were localized along the paths together with transition states corresponding to the formation of a C−C bond between the C_2H_2 and the C_4H_4 units. The insertion process appears to be 13.96 kcal/mol exothermic for Y, slightly endothermic for Zr and Nb by 3.24 and 5.01 kcal/mol, respectively. The process is sensibly exothermic, by 38.2 kcal/mol, in the case of Mo, as expected, due to the weak interaction existing in the reacting complex **IV**. The energy barrier relative to the formation of the transition state connecting intermediates **IV** and **V** amounts to 12.32 kcal/mol for Y, 16.67 kcal/mol for Zr, 28.79 kcal/mol for Nb, and 12.5 kcal/mol for Mo. For all the localized transition states, both the check of the vibrational mode associated to the imaginary frequency and the IRC calculation confirmed that the transition-state structures correspond to the insertion of the acetylene into the C−M bond of the MC_4H_4 moiety to pass from **IV** to **V**.

3.6. Benzene Formation and Desorption. As a last step, benzene formation occurs via reductive elimination of the C_6H_6 bidentate ligand from the metallacycloheptatriene, MC_6H_6, complex through the formation of the final intermediate, **VI**, appearing in the catalytic cycle. To this step is associated an energy gain of 42.86, 39.89, 28.29, and 30.81 kcal/mol for Y, Zr, Nb, and Mo, respectively. The energy barrier that is necessary to overcome in order to obtain the final adduct, $M-C_6H_6$, is very low, about 2 kcal/mol, for Y. The geometrical structure of the corresponding transition state, indeed, is only slightly different from the MC_6H_6 reactant, as shown by the variation in the M−C and C−C distances. The height of the barrier is 8.64 and 13.36 kcal/

(59) Ferrari, A. M.; Giordano, L.; Rösch, N.; Heiz U.; Abbet, S.; Sanchez, A.; Pacchioni, G. *J. Phys. Chem.* **2000**, *104*, 10612.
(60) Hardesty, J. H.; Koerner, J. B.; Albright, A. T.; Lee, G. Y. *J. Chem. Soc.* **1999**, *121*, 6055.

mol for Zr and Mo, respectively, and corresponds to more significant changes in geometrical parameters. It is noteworthy that the transition state and final benzene complex of Zr are more stable in a triplet state and a spin crossing between singlet and triplet surfaces occurs. Finally, the height becomes 23.79 kcal/mol for the transition state corresponding to the formation of $Nb-C_6H_6$ from the NbC_6H_6 intermediate. Moreover, in this case, new spin crossings occur before and after the transition state formation, lowering the energy barrier for the process.

In the equilibrium geometry, benzene is slightly distorted with respect to the free molecule in the Y and Zr adducts. Indeed, the C−M distances are different among them and some C atoms are slightly tilted upward with a loss of planarity. The molecule, instead, lies flat in the Nb complex and is detached yet in the case of Mo. The computed corresponding interaction energies are 25.19 kcal/mol for Y, 34.23 kcal/mol for Zr, and 24.65 kcal/mol for Nb, while for Mo, once formed, benzene promptly desorbs since it is unbound. As a consequence, for Y, benzene release is the rate-determining step of the overall process.

Summary and Conclusions

We have performed a theoretical investigation of cyclomerization of acetylene to give benzene mediated by the bare neutral metal atoms from the left-hand side of the 4d series. The results obtained here can serve as a first test of the catalytic ability of the considered metals in view of further studies, which we planned, of less simplified catalytic systems for the same metal atoms.

The overall $M + 3C_2H_2 \rightarrow MC_6H_6$ process appears to be highly favored thermodynamically for all the neutral metal atoms considered here and includes three individual steps that imply overcoming an energy barrier. All the possible alternative routes toward benzene formation have been examined, and the possibility that three acetylene molecules isomerize in a concerted way to give benzene has been ruled out, as well as the formation of a metal−cyclobutadiene complex. Benzene is formed through the insertion of the third activated acetylene molecule into the metal−carbon σ bond of the metallacyclopentadiene complex to give a MC_6H_6 metallacycle followed by reductive elimination. All the minima are stable, and the transition states in their ground states lie below the reactant dissociation limit. The combined thermodynamic and kinetic analysis of the process indicates that Y, Zr, and Nb can be considered good candidates for the cyclization of acetylene to give benzene, whereas the situation is more critical for Mo.

Main differences among the behaviors of Y, Zr, Nb, and Mo concern the interplay between surfaces of different multiplicity, the stability of intermediates, and the barrier heights for the transition states connecting them. The reaction evolves along the low-spin doublet surface, and all the localized stationary points along the excited quartet spin state always lie higher in energy. Formation of all the intermediates along the path takes place with an energy gain, and barrier heights for transition states are low, particularly for the last step of the reaction that leads to the formation of the benzene−metal complex. Due to low energy barriers found along the pathway for Y, the final benzene release is just the rate-determining step. The picture is less favorable for Zr. Indeed, the high stability of the bis-acetylene complex is associated to a very high energy barrier for the interconversion into the metallacycle complex that also appears to be the rate-determining step. Moreover, formation of the next intermediate along the path is endothermic. Multiple crossings between the singlet and triplet spin surfaces occur even if reactants and products have the same multiplicity. For Nb, the reaction evolves initially, until activation of the first acetylene molecule, along the surface for the first quartet excited state. Also, the transition states associated to the interconversion between intermediates **II** and **III** and between intermediates **V** and **VI** have a quartet ground state, whereas all the other stationary points are more stable in a doublet spin state. All the minima are highly stabilized, and therefore, the barrier for the interconversion from one isomer to another is quite high, being the formation of the metallacyclopentadiene the rate-determining step. Formation of intermediates **III** and **V** are computed to be slightly endothermic, while the critical step of activation of the third acetylene molecule takes place with a considerable energy gain. The reaction occurs completely along the path for the excited low-spin state in the case of Mo, and only final Mo−benzene adducts possesses the same multiplicity of reactants since the Mo atom is unbound. All the intermediates are less stabilized in comparison with Y, Zr, and Nb, and the involved transition states are associated to quite low energy barriers. It is worth noting that the third C_2H_2 molecule interacts weakly with the MoC_4H_4 unit even if the formed complex is stable enough to isomerize into the next metallacycle complex. The final step of the reaction that is detachment of the benzene ligand from the metal requires a reasonable amount of energy for Y, Zr, and Nb and promptly occurs in the case of Mo that is unbound.

Our study highlights the possible occurrence of spin crossings between surfaces of different multiplicity, even if to better characterize spin crossing points and to determine their real influence on the course of the considered reactions further detailed studies are needed. Work is in progress yet in this direction.

Acknowledgment. Financial support from the Università degli Studi della Calabria and MIUR is gratefully acknowledged.

IC051281K